



Statistical properties of image pixel brightness from the onboard optical location system

Andrei Sergeevich Solonar ^{*1}, Sergei Viktorovich Tsuprik ², Petr Aleksandrovich Khmarskiy ³

¹ Military Academy of the Republic of Belarus, Belarus, andssnew@yandex.ru

² Military Academy of the Republic of Belarus, Belarus, Serhio.Observer@yandex.ru

³ Institute of Applied Physics of the National Academy of Sciences of Belarus, Belarus, pierre2009@mail.ru

Cite this study: Solonar, A. S., Tsuprik, S. V., & Khmarskiy, P. A. (2023). Statistical properties of image pixel brightness from the onboard optical location system. *Advanced UAV*, 3 (2), 142-152

Keywords

Image processing
Unmanned aerial vehicle
Optical location system
Image pixel brightness

Research Article

Received:03.08.2023
Revised:18.10.2023
Accepted:13.11.2023
Published:17.11.2023

Abstract

The statistical properties of image pixel brightness were investigated to provide a rationale for the choice of the necessary mathematical image model. Video recordings of the ground situation, obtained from the onboard optical-location system of an unmanned aerial vehicle, were generated and analyzed. The requirements for a mathematical model of brightness under ground-based background-target conditions were formulated. Based on these requirements, a semi-Markov model of brightness with Poisson moments of transition from one state to another was proposed to describe pixel brightness. The adequacy of the proposed model in describing pixel brightness has been verified.



1. Introduction

Many scientific publications [1-9] discuss the effective utilization of information from the onboard optical-location system (OLS) for tracking ground objects. These objects encompass civil and military ground transportation, people, infrastructure, and more [10-19]. Tracking in OLS becomes challenging due to the observation of objects against complex and diverse backgrounds such as road surfaces, landscapes, vegetation, and other ground objects. Additionally, the ground background-target situation often involves multiple objects simultaneously within the OLS frame, making manual tracking by operators difficult. To address multi-target situations, automating the tracking process based on onboard radar data proves to be effective. Common approaches for automation include contour analysis, reference point selection, extreme-correlation analysis, and neural network algorithms [1,2,6,7]. However, their effective application in ground-based background-target scenarios remain a relevant issue, given the diversity of acquired images. As a result, various accepted mathematical models of images have emerged to tackle this diversity [2,6].

This paper explores the statistical properties of image pixel brightness and aims to select a highly suitable mathematical model. The analysis of video recordings from the airborne optical-location system is presented, which captures ground background-target situations. This analysis enables the formulation of requirements for the chosen mathematical model.

2. Material and Method

The image formed by a video sensor is the result of registering radiant energy (brightness) coming from the observed scene and converting it into electrical signals. Matrices on charge-coupled devices (CCDs) are widely used as video sensors [1,7]. The CCD sensor uses a rectangular lattice of nodes where electrons are collected

(Figure 1). The distribution of light flux brightness along the rectangular coordinates of the CCD matrix (x, y) at the moment of time t can be represented by a two-dimensional function of the form Equation 1:

$$f(x, y, t) = \int_0^\infty C(x, y, \lambda, t) S(\lambda) d\lambda \quad (1)$$

where $0 \leq C(x, y, \lambda, t) \leq C_{\max}$ is the function of brightness distribution on rectangular coordinates of CCD matrix (x, y) depending on the wavelength λ of light flux components at the moment of time t ; C_{\max} is the maximum brightness; $S(\lambda)$ - spectral sensitivity of the video sensor.

The geometric dimensions of a rectangular grating are constrained by the characteristics of the imaging system (optical system) and are different from zero $0 \leq x \leq l_x, 0 \leq y \leq l_y$. The function $f(x, y, t)$ represents an analog image and is bounded in the rectangular area $l_x \times l_y$. To realize digital processing, the continuous image $f(x, y, t)$ is converted into a digital image. The process of converting a continuous image into a discrete image is called discretization, and the image is discretized.

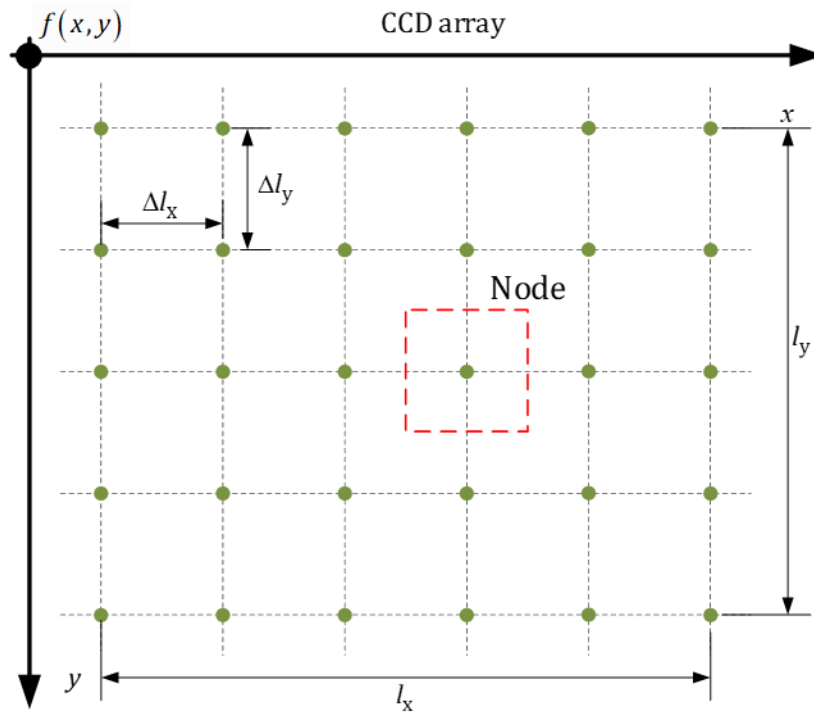


Figure 1. Representation of an image formed by a rectangular CCD matrix.

A color discretized image \mathbf{f}_k with frame number k , formed at time t , is a set of three rectangular matrices of size L_x per L_y red (r), green (g) and blue (b) colors (Equation 2):

$$\mathbf{f}_k = \{ \mathbf{f}_k^r, \mathbf{f}_k^g, \mathbf{f}_k^b \} = \{ \mathbf{f}_k^c \}_{c=1}^3 \in \Lambda_f, \quad \mathbf{c} = \{ r=1, b=2, g=3 \} \quad (2)$$

Where $\mathbf{f}_k^c = \{ \mathbf{f}_{kij}^c \}_{i=0, j=0}^{i=L_y-1, j=L_x-1}$ is the general designation of the rectangular image matrix of red color at $c=1$ (r), green at $c=2$ (g) and blue at $c=3$ (b); Λ_f are the set of points in the observation space belonging to the image $\mathbf{f}_k^c \in \Lambda_f$; $i=0 \dots L_y-1, j=0 \dots L_x-1$ are row and column numbers of the matrices; \mathbf{f}_{kij}^c is the general notation of the pixel number (i, j) of the discretized image of red at $c=1$, green at $c=2$ and blue at $c=3$.

Brightness values in color channels $\mathbf{f}_{kij}^r, \mathbf{f}_{kij}^g, \mathbf{f}_{kij}^b$ are formed independently of each other and are complexed in the process of further processing. Brightness of a pixel of the frame image \mathbf{f}_{kij}^c can take integer values

in the range of $\mathbf{f}_{kij}^c \in 0...255$. The number of pixels (nodes) in the CCD matrix is defined by the rectangular area $l_x \times l_y$ (Equation 3):

$$L_x = l_x / \Delta l_x, \quad L_y = l_y / \Delta l_y \quad (3)$$

where $\Delta l_x = l_x / L_x, \Delta l_y = l_y / L_y$ is the distance between the pixels of the CCD matrix along the coordinate x and y .

As a rule, the brightness values of image pixels \mathbf{f}_k are known only at the moment of frame time k , and the regularities of their changes in time are not known and are random. This is primarily due to the constantly changing background-target environment, where the observed objects move both due to their own motion and due to the movement of the optical axis of the OLS. In this regard, it is convenient to use a mathematical model of the form to describe the brightness of the image (Equation 4):

$$\mathbf{f}_{(k+1)ij}^c = \mathbf{H}\alpha_{(k+1)ij}^c + \mathbf{w}_{(k+1)ij}^c \quad (4)$$

where $\mathbf{H} = \begin{bmatrix} 1 & 0 \end{bmatrix}$ is the static vector of recalculation of changes in the state vector into changes in the vector of observed parameters; $\alpha_{(k+1)ij}^c$ is the vector of brightness state of the (ij) -th pixel on the $(k+1)$ -th frame in the each color channel \mathbf{c} ; $\mathbf{w}_{(k+1)ij}^c$ are the uncorrelated Gaussian samples of brightness fluctuations in the each color channel (c) .

The state vector $\alpha_{kij}^c = \begin{bmatrix} \Theta_{kij}^c & \mathbf{V}_{\Theta_{kij}^c}^c \end{bmatrix}^T$ may include the brightness of a pixel of the image of some object Θ_{kij}^c and its rate of change $\mathbf{V}_{\Theta_{kij}^c}^c$. In such a case, the state vector can be represented as a Markov model (Equation 5):

$$\alpha_{(k+1)ij}^c = \mathbf{B}\alpha_{kij}^c + \mathbf{S}\eta_{(k+1)ij}^c \quad (5)$$

where $\mathbf{B} = \begin{bmatrix} 1 & \Delta t \\ 0 & 1 \end{bmatrix}$ is the dynamic matrix of conversion of the state vector from k to $(k+1)$ -th frame; $\mathbf{S} = \begin{bmatrix} \Delta t^2/2 & \Delta t \end{bmatrix}^T$ is the vector of linear transformation over samples of uncorrelated white Gaussian noise; $\eta_{(k+1)ij}^c$ are the samples of uncorrelated white Gaussian noise with zero mathematical expectation and unit variance for the (ij) -th pixel.

Nevertheless, the issue of choosing an adequate mathematical model in the current conditions remains relevant. This is due to the fact that the Markov model (Equation 5) does not take into account possible jump-like changes in brightness, which may occur when observing highly maneuverable objects observed against a complex heterogeneous background. Thus, in order to select the most appropriate mathematical model for brightness description, studies of its statistical properties were conducted. The studies included estimation of the law of pixel brightness distribution, their numerical parameters, and autocorrelation properties. Also, in order to assess the influence of discontinuous changes in brightness and the possibility of taking them into account, the dynamic stability of the brightness of the image pixels was assessed (stationarity assessment).

3. Results and Discussion

The research was conducted in accordance with the developed methodology, which consists of the following steps:

Step 1. A data bank containing the same type of video recordings for given surveillance conditions shall be formed.

Step 2. The images belonging to the objects of interest are extracted from the data bank. Then the dependence of pixel brightness variation on the frame number is calculated.

Step 3. The brightness distributions of images are analyzed using the histogram method. The brightness distributions of individual pixels are analyzed. Autocorrelation functions (ACF) are constructed and analyzed.

Step 4. The dynamic stability of the process of pixel brightness change is estimated (stationarity estimation).

In order to carry out experimental studies following the described methodology, an experimental study program was developed, as depicted in Figure 2. The program complex consists of several components, including a data bank, an object image extraction device, a pixel brightness analysis device, and an assessment of dynamic stability.

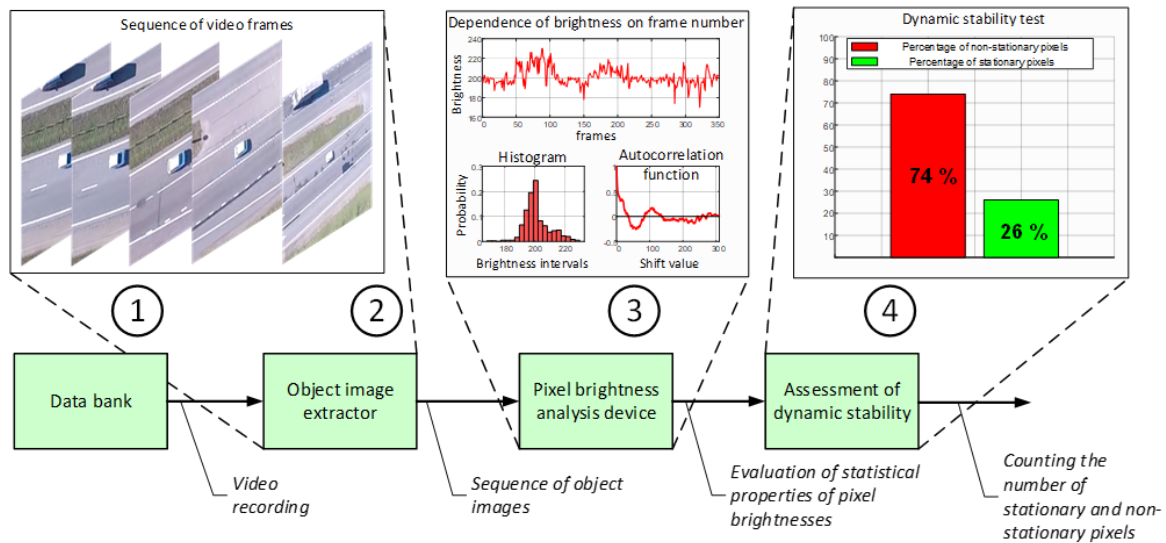


Figure 2. The structural scheme of the program complex of experimental research.

The data bank of object images, consists of 18 records. The total size of the analyzed sample was more than 100000 brightness samples. The sizes of object images are fixed and amounted to 32x32 pixels. It is considered that during the observation process the sizes of the object images remain unchanged. The objects are observed from different angles due to their own motion, UAV motion and rotation of the UAV. The background has a complex structure as it includes various elements such as a road with markings, vegetation patches, and other passing vehicles. It is considered that part of the background pixels belongs to the images of objects and makes up no more than 10% of the total number of pixels. Shooting was carried out during daylight hours in conditions of good visibility and absence of interfering factors (rain, snow, fog, etc.). Recording was carried out with a resolution of 1920x1080 pixels and 29 frames per second. To ensure the objectivity of the analysis, the recordings were made for the same type of observation conditions by one camera.

Extraction of object images from video records is performed sequentially on each frame. An example of images extracted from the data bank is shown in Figure 3. The operator manually selects the area on the image belonging to the object by issuing a target designation on the image of the video recording frame.

Object sizes throughout the whole recording should not change significantly, and are considered equal to the image sizes on the first frame. Selected images of the object are memorized in a time-ordered manner into a buffer for further processing.

The results of the analysis of pixel brightness distribution and their correlation properties according to the brightness slices are shown in Figure 4. It was performed by the histogram method. The number of grouping intervals for histogram construction was 50. The obtained histograms show that the pixel and image brightness distributions have a multimode character, which means that the distribution parameters change in the process of observation. Basically, changes in the distribution parameters occur due to changes in the orientation of the observed object in space, which leads to distortion of its image.

To evaluate correlations between brightness values at different moments of time, the ACF of image brightness was analyzed for all pixels over the entire observation interval. It follows from the analysis that the ACF can be approximated by an exponential function. Since the correlation time can be significantly different for each individual pixel, the correlation time should be chosen as the average of all pixels in the image.

The dynamic stability was evaluated using the Kwiatkowski-Phillips-Schmidt-Shin test [20]. This test is widely used in economics for building regression models [20]. The choice of this test is due to its high accuracy and independence from the distribution law. Figure 5 shows the results of stationarity intervals for one pixel in 3 RGB color channels. The graphs show that there are about 10 stationarity intervals of different lengths on the observation interval. It follows that the stationarity condition for this pixel is not fulfilled.

Similarly, the results for all pixels in the image were obtained and the pixels that are non-stationary were counted. The results of this counting are shown in Figure 6. It can be seen that 74% of the image pixels that make up the data bank are non-stationary. The estimation of the duration of the stationarity intervals indicates similarities with the exponential law (Figure 6). The well-known statistical criterion of Pearson's chi-square test of agreement was used to evaluate the degree of correspondence.



Figure 3. Conditions of ground objects observation according to onboard optical location data: a, b - civilian vehicles on the highway; c, d - military vehicles on the march.

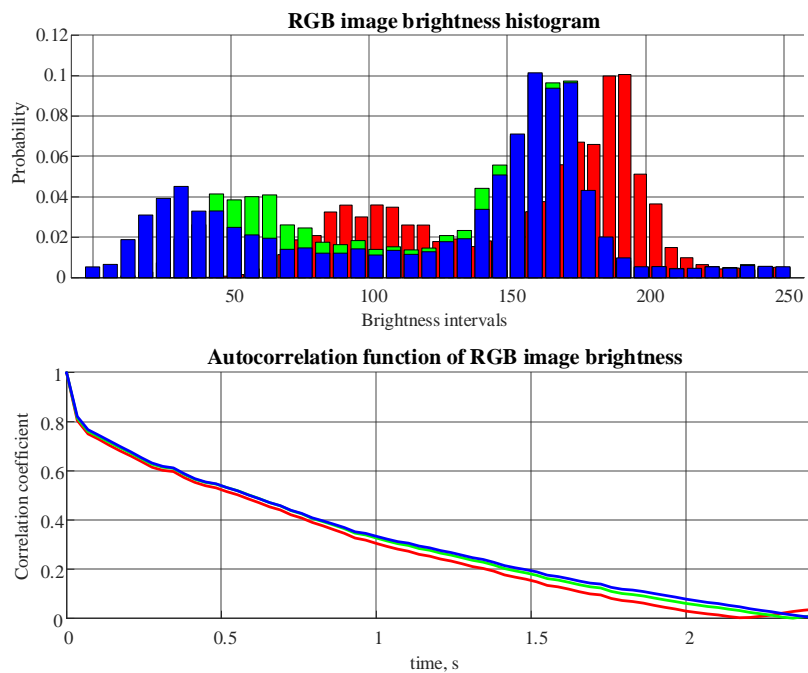


Figure 4. Brightness histograms, autocorrelation function of ground object image brightness in three RGB color channels.

Result of stationarity intervals selection

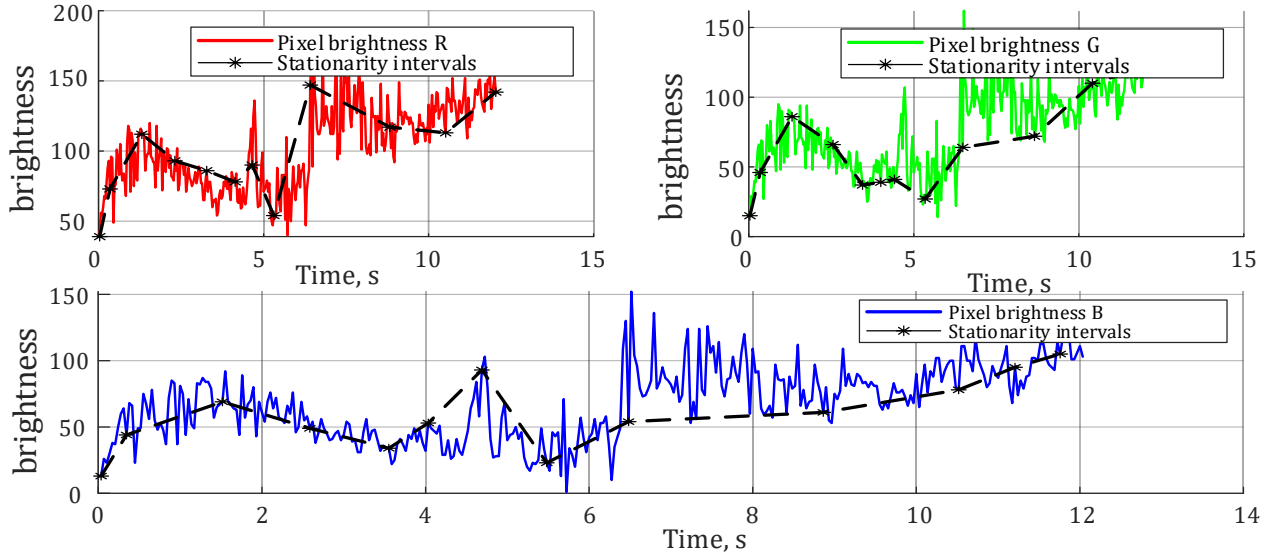


Figure 5. Example of selection of pixel brightness stationarity intervals.

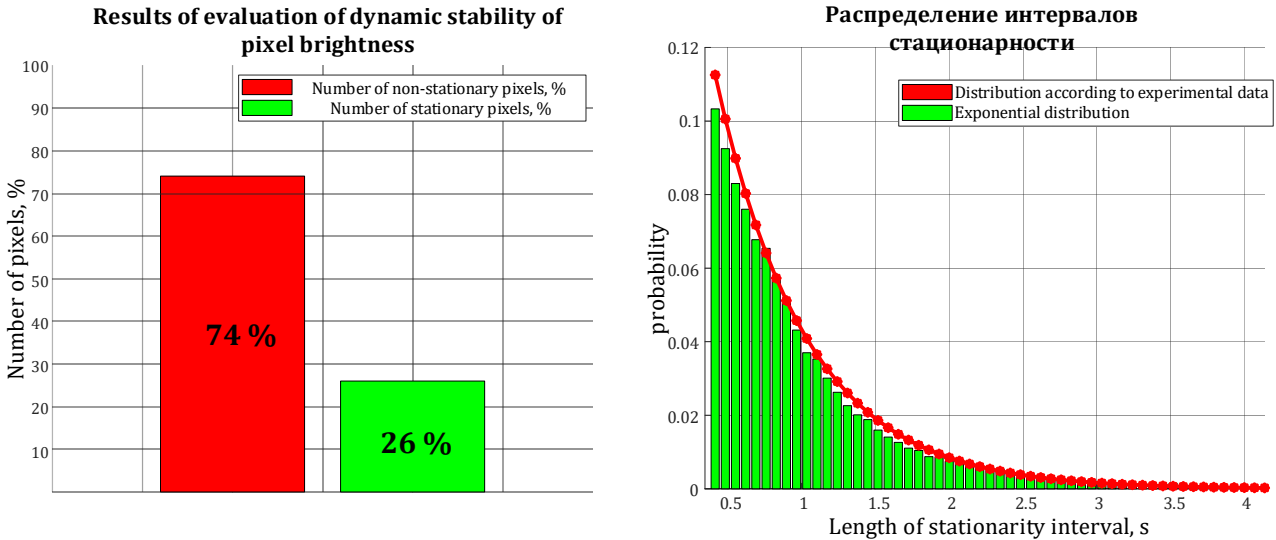


Figure 6. Results of estimation of dynamic stability and distribution of interval intervals of pixel brightness stationarity.

As a result, it was found that the obtained distribution of stationarity intervals with confidence probability not less than 0.9 corresponds to the exponential law. The correspondence of the durations of time intervals to the exponential law indicates that the process of brightness variation in time can be obtained using a Markov sequence model with continuous time given by a Poisson flow of events.

In [8], this approach is called semi-Markovian and is used to build models of maneuvering targets motion from radar data. The expression for the semi-Markovian model of the setting influence has the form (Equation 6):

$$\alpha_{(k+1)ij}^c = B\alpha_{kij}^c + S\left(\eta_{(k+1)ij}^c + \mu_{(k+1)ij}^c\right) \quad (6)$$

where $\mu_{(k+1)ij}^c$ is the deterministic brightness value of the (ij) -th pixel.

The brightness values $\mu_{(k+1)ij}^c$ for a color depth of 8 bits vary in a range $\mu_{(k+1)ij}^c \in 0...255$ at random moments of time determined by a Poisson flow of events. The time moments between the change of states $\mu_{(k+1)ij}^c$ are called

stationarity intervals $\Delta t_{tr(s+1)}$, the distribution of which is described by an exponential law. The expression for the generation of the stationarity interval $\Delta t_{tr(s+1)}$ has the form (Equation 7):

$$\Delta t_{tr(s+1)} = -\frac{1}{\lambda_{tr(s+1)}} \ln(r_s) \tag{7}$$

where $\lambda_{tr(s+1)}$ is the intensity of the Poisson flow of events at the $(s+1)$ -th time interval, where $s = 1, 2, \dots, N_s$; N_s is the total number of time intervals; r_s is the uniformly distributed random variable from 0 to 1.

Since the number of stationarity intervals depends only on the total observation time and does not depend on the time instant $t_{(k+1)}$, the Poisson flow is considered stationary and its intensity $\lambda_{tr(s+1)}$ is constant and equal to $\lambda_{tr(1)} = \lambda_{tr(2)} \dots \lambda_{tr(s)} = \lambda_{tr}$.

Taking into account expression (Equation 7), the moment of time of change of states $\mu_{(k+1)ij}^c$ at the $(s+1)$ -th time interval according to the Poisson flow has the form (Equation 8):

$$t_{tr(s+1)} = t_{tr(s)} + \Delta t_{tr(s+1)} \tag{8}$$

where $t_{tr(s)}$ - is the value corresponding to the s -th time interval.

The results of checking the adequacy of the mathematical model (Equation 6) are presented in detail in [10], and some of them are shown in Figure 7a, from which it follows that the distribution of stationarity intervals obtained from the results of mathematical modeling corresponds to the experimental data contained in the data bank. The degree of correspondence is confirmed by Pearson's chi-square criterion of agreement with a confidence level not lower than 0.9. Figure 7b shows the estimates of ACF obtained from the results of modeling and from the contents of the data bank. It can be seen that the shape of the ACF and the correlation time have close values.

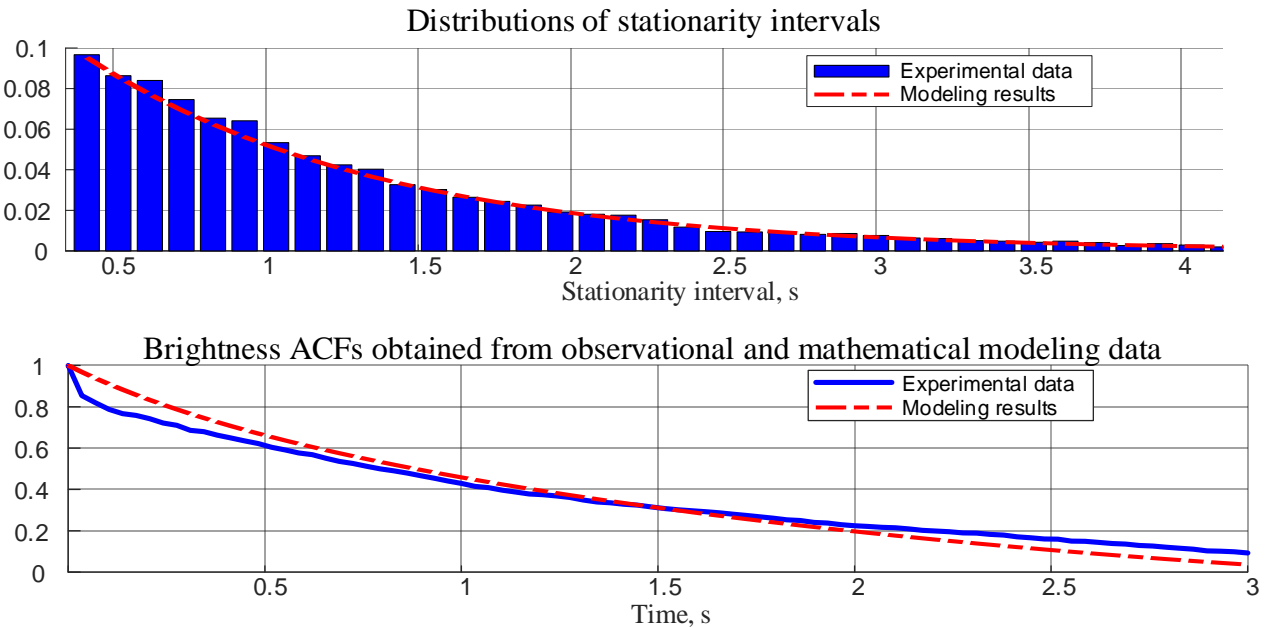


Figure 7. Results of comparison of distributions of stationarity intervals and brightness ACF obtained from observations and mathematical modeling data.

In accordance with the methodology [9], estimates of the confidence interval of the correlation time $I_{\hat{t}_0}$ and brightness intensity $I_{\hat{\lambda}_{tr}}$ were obtained from the data contained in the data bank, as well as their point estimates from the modeling results. The degree of compliance of the modeling results was determined by

checking whether the point estimates fall within the confidence interval $I_{\hat{\tau}_0}$ and $I_{\hat{\lambda}_{tr}}$ with probability 0.9 and 0.95. The results of the verification are summarized in Table 1.

Table 1. Point and interval estimates of correlation times τ_0 and intensities λ_{tr} .

Model parameters	Point estimate $\hat{\tau}_0$ and $\hat{\lambda}_{tr}$		Interval estimation $I_{\hat{\tau}_0}$ and $I_{\hat{\lambda}_{tr}}$			
	Data Bank	Mat. modeling	Left boundary of the confidence interval		Right boundary of the confidence interval	
			0,9	0,95	0,9	0,95
Correlation time τ_0	0,558 – 4,026	0,562 – 3,955	0,542 – 3,945	0,538 – 3,929	0,574 – 4,107	0,577 – 4,11
Intensity of transitions λ_{tr}	0,654 – 0,9	0,674 – 0,919	0,629 – 0,876	0,624 – 0,871	0,679 – 0,925	0,683 – 0,93

As a result, with confidence probability not lower than 0.9 and error not more than 5 %, the estimates of correlation time and intensity of transitions obtained from the modeling results correspond to similar estimates obtained from the experimental data (Table 1). Thus, the obtained results of mathematical modeling confirm a high degree of adequacy of the semi-Markov model used to describe the brightness of images of ground objects. To assess the quality of the description of the observed process proposed by the semi-Markov model (Equation 6), a comparative analysis was carried out. The Markov model (Equation 5) is chosen as an alternative model used to describe images of moving objects. The main indicator of the model quality is the value of the total standard deviation of the brightness from the true value (non-convexity) of the setting and perturbing influences.

The results of estimation of the quality of the observed process description on the example of one pixel for the Markov model, in which the regular component of the setting influence is represented by a polynomial model of the 0th order, are shown in Figure 8.

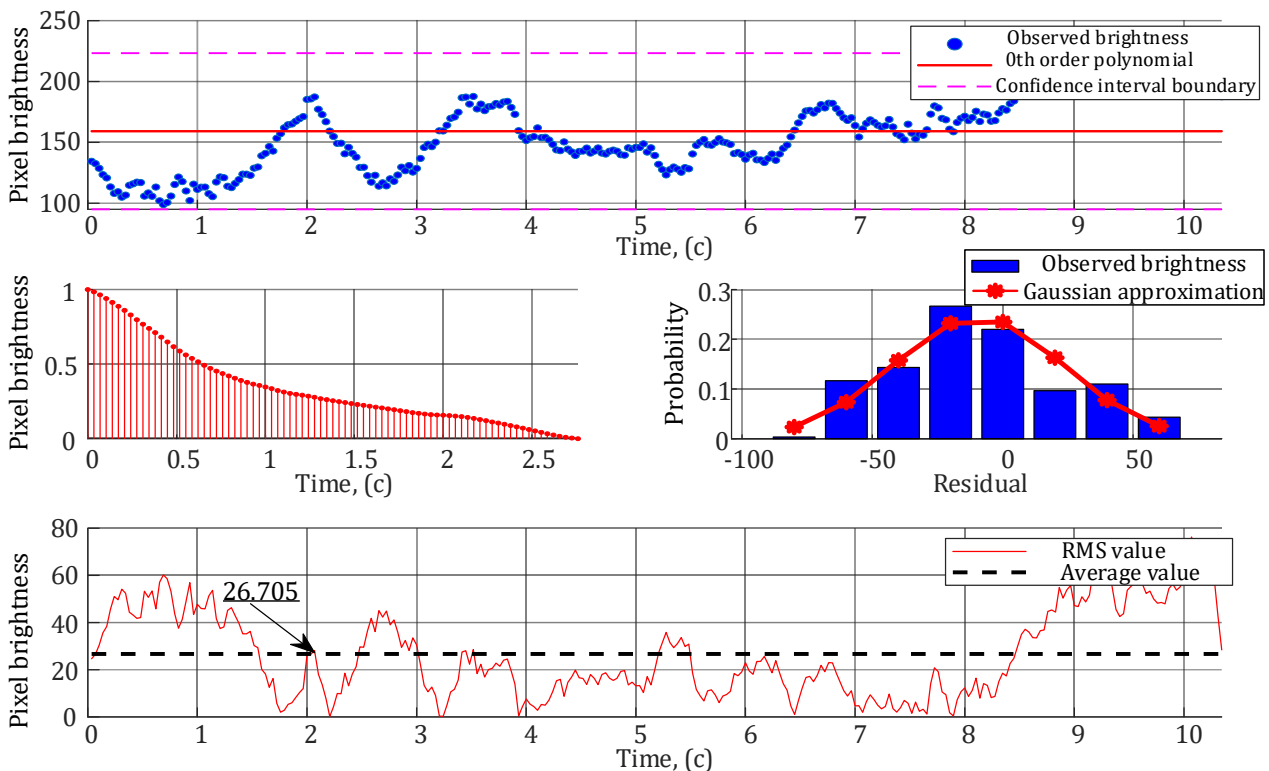


Figure 8. Results of quality assessment of the description of the observed process using the Markov model with the setting influence in the form of a 0-th order polynomial.

Figure 8a show the time dependence of the observed brightness. From these data, the brightness discrepancy is calculated, indicating the degree of fit of this model to the observed process. The ACF of the mismatch and the histogram of the distribution are shown in Figure 8b, 8c. It can be seen that the correlation time of the mismatch is of the order of 2.5 s, indicating a high correlation preserved after subtracting the regular

component of the model from the process. The obtained estimation of the distribution of the inconsistency with a confidence probability not lower than 0.9 showed non-compliance with the normal law of distribution. The dependence of the RMS of the observation on the 0-th order polynomial model in Figure 5d indicates a low quality of the brightness description, maintaining a large value of the mean RMS - 26.7.

The results of evaluating the quality of the description of the observed process using the semi-Markov model are shown in Figure 9, where the process of describing the observed process within a limited time interval (stationarity interval) is depicted. Figures 9b, 9c show that the magnitude of the observations is practically not correlated, as evidenced by the close to zero value of the correlation time of the obtained ACF estimation. The histogram of the discrepancy distribution (Figure 9c) follows the normal law with a confidence level of 0.9.

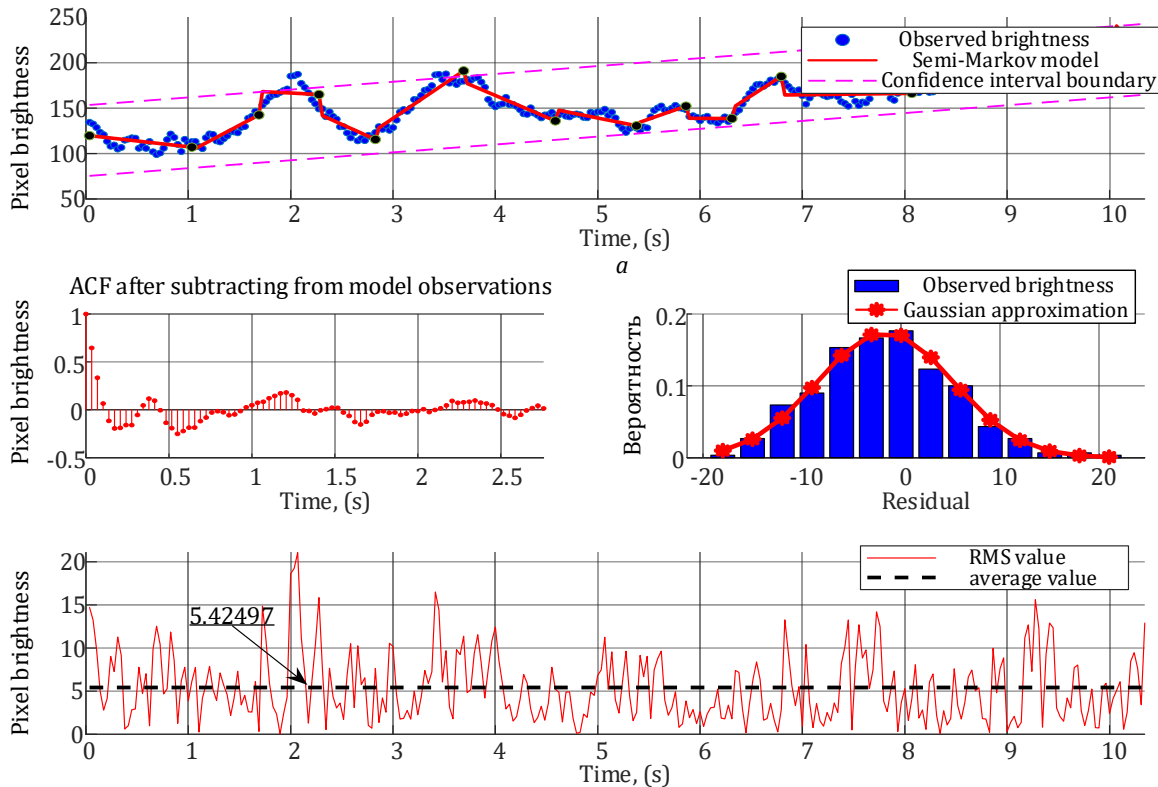


Figure 9. Results of quality assessment of the description of the observed process using a semi-Markov model.

The given RMS dependence in Figure 9 shows that the mean value was 5.4, which is less by a factor of 1.5-1.9 compared to the Markov model (Equation 5).

4. Conclusion

According to the proposed research methodology on the statistical properties of pixel brightness in images obtained from an airborne optical location system, the mathematical model for pixel brightness in ground object images should possess the following properties:

1. The law of pixel brightness distribution is unknown and exhibits a multi-modal structure.
2. The change in pixel brightness over time is primarily non-stationary (approximately 74%) and demonstrates properties of a dynamic system, with parameters varying over time.
3. The durations of stationary intervals follow an exponential distribution, and state transitions occur randomly according to the Poisson distribution.
4. The autocorrelation properties of pixel brightness over time can be described by an exponential ACF (Autocorrelation Function), where the correlation time corresponds to the average correlation time in each pixel of the object image.

A semi-Markov model of pixel brightness was proposed [10], which differs from the Markov model by the possibility of adequate description of images of maneuvering objects. The application of the semi-Markov model allowed us to reduce the total RMS of the brightness discrepancy compared to the Markov model, in which the regular component is represented by a polynomial model of the 0th order by 1.5-1.9 times.

Acknowledgement

This study was partly presented at the 7th Advanced Engineering Days [21].

Funding

Research was carried out with the support of a grant from the Belarusian Republican Foundation for Fundamental Research (project No. F23M-103).

Author contributions

Andrei Sergeevich Solonar: Substantiation of the research concept, formulation of ideas, research goals and objectives, development of methodology and research model; **Sergey Viktorovich Tsuprik:** Collection and systematization of data, computer and mathematical modeling, comparative analysis, writing the text of the manuscript; **Petr Aleksandrovich Khmarski:** Generalization and interpretation of the results of the study, editing the text of the manuscript, working with graphic material.

Conflicts of interest

The authors declare no conflicts of interest.

References

1. Ali, B., Sadekov, R. N., & Tsodokova, V. V. (2022). A review of navigation algorithms for unmanned aerial vehicles based on computer vision systems. *Gyroscopy and Navigation*, 13(4), 241-252. <https://doi.org/10.1134/S2075108722040022>
2. Artemiev, V. M., Naumov, A. O., & Kohan, L. L. (2014). Image processing in passive survey and search optoelectronic systems. Minsk, Belaruskaya navuka. ISBN 978-985-08-1657-3
3. Artemiev V. M., Naumov A. O., & Kohan L. L. (2010). Point objects detection in the case of uncertainty. *Informatika = Informatics*, 2, 15–24.
4. Mueller, K., Atman, J., & Trommer, G. F. (2019). Combination of wide baseline image matching and tracking for autonomous uav approaches to a window. *Gyroscopy and Navigation*, 10, 206-215. <https://doi.org/10.1134/S2075108719040138>
5. Hecker, P., Angermann, M., Bestmann, U., Dekiert, A., & Wolkow, S. (2019). Optical aircraft positioning for monitoring of the integrated navigation system during landing approach. *Gyroscopy and Navigation*, 10, 216-230. <https://doi.org/10.1134/S2075108719040084>
6. Solonar, A. S., & Khmarski, P. A. (2021). Main problems of trajectory processing and approaches to their solution within the framework of multitarget tracking. In *Journal of Physics: Conference Series*, 1864(1), 012004. <https://doi.org/10.1088/1742-6596/1864/1/012004>
7. Solonar, A. S., Khmarskiy, P. A., Mihalkovskiy, A. A., & Tsuprik, S. V. (2018). Features of trajector measurement coordinates and parameters of movement of ground objects in on-board optical-location systems. In *2018 25th Saint Petersburg International Conference on Integrated Navigation Systems (ICINS)*, 1-5. <https://doi.org/10.23919/ICINS.2018.8405853>
8. Farina, A., & Studer, F. A. (1985) *Radar data processing: Vol. 1 – Introduction and tracking*. ISBN 0863800262.
9. Kosachev, I. M., Nefedov, D. S. (2015). Methods of calculation of reability and accuracy indicators of the estimated tactical and technical characteristics of weapons, military and special equipment. *Vest. Military Academy, Republic of Belarus*, 1, 107–134.
10. Solonar, A. S., Tsuprik, S. V., & Khmarski, P. A. (2023). Semi-Markov model of brightness change of the ground object image formed by the optical-location system. *Vest. Military Academy, Republic of Belarus*, 1, 97 – 107.
11. Akhloufi, M. A., Castro, N. A., & Couturier, A. (2018). UAVs for wildland fires. In *Autonomous systems: Sensors, vehicles, security, and the Internet of Everything*, 10643, 134-147. <https://doi.org/10.1117/12.2304834>
12. Jordan, S., Moore, J., Hovet, S., Box, J., Perry, J., Kirsche, K., ... & Tse, Z. T. H. (2018). State-of-the-art technologies for UAV inspections. *IET Radar, Sonar & Navigation*, 12(2), 151-164. <https://doi.org/10.1049/iet-rsn.2017.0251>
13. Scherer, J., Yahyanejad, S., Hayat, S., Yanmaz, E., Andre, T., Khan, A., ... & Rinner, B. (2015, May). An autonomous multi-UAV system for search and rescue. In *Proceedings of the First Workshop on Micro Aerial Vehicle Networks, Systems, and Applications for Civilian Use*, 33-38. <https://doi.org/10.1145/2750675.2750683>
14. Mittal, M., Mohan, R., Burgard, W., & Valada, A. (2019). Vision-based autonomous UAV navigation and landing for urban search and rescue. In *the International Symposium of Robotics Research*, 575-592. https://doi.org/10.1007/978-3-030-95459-8_35

15. Lu, Y., Xue, Z., Xia, G. S., & Zhang, L. (2018). A survey on vision-based UAV navigation. *Geo-spatial Information Science*, 21(1), 21-32. <https://doi.org/10.1080/10095020.2017.1420509>
16. Schleiss, M. (2019). Translating aerial images into street-map-like representations for visual self-localization of UAVs. *The International Archives of the Photogrammetry, Remote Sensing and Spatial Information Sciences*, 42, 575-580. <https://doi.org/10.5194/isprs-archives-XLII-2-W13-575-2019>.
17. Silva Filho, P., Shiguemori, E. H., & Saotome, O. (2017). UAV visual autolocalization based on automatic landmark recognition. *ISPRS Annals of the Photogrammetry, Remote Sensing and Spatial Information Sciences*, 4, 89-94. <https://doi.org/10.5194/isprs-annals-IV-2-W3-89-2017>
18. Saranya, K. C., Naidu, V. P. S., Singhal, V., & Tanuja, B. M. (2016). Application of vision-based techniques for UAV position estimation. *International Conference on Research Advances in Integrated Navigation Systems (RAINS)*, 1-5. <https://doi.org/10.1109/RAINS.2016.7764392>
19. Masselli, A., Hanten, R., & Zell, A. (2016). Localization of unmanned aerial vehicles using terrain classification from aerial images. In *Intelligent Autonomous Systems 13: Proceedings of the 13th International Conference IAS-13*, 831-842. https://doi.org/10.1007/978-3-319-08338-4_60
20. Kwiatkowski, D., Phillips, P. C., Schmidt, P., & Shin, Y. (1992). Testing the null hypothesis of stationarity against the alternative of a unit root: How sure are we that economic time series have a unit root?. *Journal of Econometrics*, 54(1-3), 159-178. [https://doi.org/10.1016/0304-4076\(92\)90104-Y](https://doi.org/10.1016/0304-4076(92)90104-Y)
21. Solonar, A. S., Tsuprik, S. V., & Khmarskiy, P. A. (2023). Statistical properties of image pixel brightness from the onboard optical system. *Advanced Engineering Days (AED)*, 7, 172-174.



© Author(s) 2023. This work is distributed under <https://creativecommons.org/licenses/by-sa/4.0/>